A hybrid of GNSS remote sensing and ground-based laser technology for geo-referenced surveying in mining

Amar Prakash*, Aniket Verma, Anand Sharma, Prerna Jaiswal and Sujit K. Mandal

Central Institute of Mining and Fuel Research, Barwa Road, Dhanbad 826 015, India

Rapid, precise and frugal surveying is a strategic factor in the present mechanized mining environment owing to rapid surface profile transformation in a short period. Determination of global coordinates with high accuracy using the satellite-based global navigation satellite system (GNSS) has been studied in the mining arena and is gradually becoming an essential component. A case study of Khanak Stone Mine, Haryana, India, is discussed here, highlighting the combination of GNSS system and terrestrial laser scanner for the preparation of a surface profile of a rugged terrain with the key objective to determine the precise *in situ* rock excavation in periodical phases. The actual tonnage of rock produced/ transported from the mine has been calculated by determining the *in situ* density and bulk density in the laboratory. The study reveals that this survey of approach is apt to achieve quality plan and to obtain the goal of actual tonnage of rocks excavated.

Keywords: Georeferenced surveying, hybrid technology, laser scanner, remote sensing, Stone Mine.

SCIENTIFIC collection and generation of data in the form of northing, easting and elevation to the maximum possible accuracy from the field in less time is the key objective in surveying. Quality of surveying has been improved manifold with the increase in technology. It is cumbersome to use the conventional instruments in surveying and hence inclination towards the advance survey equipment has become the need of the hour to acquire desired quality output. Conducting accurate surveys of large areas within a stipulated time frame is another pivotal factor. Keeping pace with the changing global scenario, the hybrid approach of satellite-based and land-based advanced surveying has become a promising tool in mining. Nowadays, many industries prefer surveying using advanced technology, thereby ensuring proper data generation and, in turn, precise preparation of plans and sections for perfect and in-time execution of work.

A study was conducted at Khanak Stone Mine, Haryana State Industrial and Infrastructure Development Corporation Ltd (HSIIDC), India, to determine the volume of rock excavation by laser technology. A combination of global navigation satellite system (GNSS), total station and LiDAR-based terrestrial laser scanner (TLS) was used to survey intricate terrain to obtain accurate field data.

*For correspondence. (e-mail: amar_cmri@yahoo.co.in)

Modern survey instrumentation: a backdrop

GNSS

GNSS, an outgrowth of the differential global positioning system (DGPS), bridges the gap in calculating the global coordinates of a point at the surface of the Earth by trilateration with high precision. It uses the core satellite constellations, i.e. the United States' Global Positioning System (GPS) and the Russian Federation's GLObal NAvigation Satellite System (GLONASS), the European Satellite Navigation System (GALILEO) and China's COMPASS/ Bei-Dou, India's Regional Navigation Satellite System (IRNSS) and Japan's Quasi-Zenith Satellite System (QZSS) and augmentation systems. Satellite navigation systems have becomeintegral to all applications where mobility plays an important role[1].

The GNSS receiver, consisting of an antenna and a processor, measures three-dimensional global coordinates from a minimum of four satellites with an accuracy depending on the precision of measurement from the satellites and their relative positions geometry[2]. The position is computed by the GNSS receiver through a trilateration procedure, which includes the measure of distance between the receiver and a set of satellites[3]. Dual-frequency (L1/L2) GNSS receivers for geodetic surveying are able to achieve up to 1 mm level of accuracy[4]. This eliminates the influence of the ionosphere and enhances the ambiguity resolution[5].

The amalgamation of base receiver, rover receiver and satellites, which helps mitigate orbit errors, transmission delays in the ionosphere, tropospheric errors, multipath signals and satellite and receiver clock errors, is key in acquiring precise coordinates. However, the reduction of ionospheric disturbances is still one of the unsolved issues in precise GNSS positioning[6]. Wielgosz *et al.*[7] conducted detailed research on GNSS positioning and applications in

Poland, highlighting the various functional positioning models. Several projects have been launched to promote the next generation of GNSS[8]. Also, GNSS is widely used in various domains like transportation, mapping and surveying, monitoring of the environment, weather prediction[9,10], tectonics and geodynamics[11], natural resources management, disaster warning and emergency response, and aviation, including mining[12,13]. DGPS is used in mining for planning and designing purposes, and it provides more reliable and accurate data that can be used for medium- to small-scale maps[14].

The high accuracy of GNSS has transformed the survey approaches in mining. The application area using DGPS has proven to be useful for general boundary geo-referencing and fixation if the necessary precautions are followed[15]. GNSS is not only cost-effective, but also saves enormous time compared to conventional methods[16].

TLS

Laser scanners are being widely used in several industries, including mining[17]. TLS is a ground-based survey instrument with the potential to measure millions of three-dimensional point cloud data in x, y, z format using laser beams[18,19]. In this technique, a high-frequency laser beam is emitted towards the direction of objects and a three-dimensional coordinate point is obtained based on the time of reflection, angle and intensity of the returned signals with an accuracy of 5 mm (ref. 20). Survey of inaccessible locations even in foggy and dusty environments is an advantageous quality feature of the instrument[21].

Case study

Study site

The Khanak Stone Mine is located in the northern part of Bhiwani district, Haryana. The mine lies between 28°53′36.51″–28°54′48.46″N lat. and 75°50′51.39″–75°52′50.70″E long. with a mining lease area of 258.30 ha divided into three blocks. The mountain is outcropped by exposed rocks in the majority of the locations, with a few large trees and bushes at the top of the mountain. Vivid presentation of the steep slope terrain, nearing vertical, due to old mining indicated the inaccessibility of the rocky mountain.

Need for hybrid technology

The huge demand for the quality stones of Khanak Stone Mine for large construction companies requires massive annual production. The mine, being outsourced for rock excavation, requires in-time precise surveys as payments are to be made according to actual excavation. The location of the Khanak Stone Mine was in isolation from any nearby reference coordinates. Hence, the establishment of a base station with global coordinates is the initial step to begin a survey of the mine.

The haphazard, old and abandoned mining all around the foot of the mountain further enhanced the complexity of obtaining the exact surface profile prior to new mining operations. TLS ensures accurate LiDAR-based measurement of coordinates data in northing, easting and elevation at short distances (a few centimetres) of the ground surface. The generation of huge data files bridges the gap in obtaining precise geometry of the three-dimensional ground profile. Thus, keeping in view the intricate topography, a combined satellite and ground-based survey approach was adopted to establish a new base station and baselines by GNSS and to survey the three blocks covering inaccessible areas by laser technology.

Measurement process

In order to cover the entire rugged terrain, the present study involved a systematic and scientific survey.

Establishment of base station: Establishment of the base station is essential to initiate the survey work. There were no reference coordinates in the vicinity of the study area. Guidelines have been framed by the Survey of India (SoI) for the duration of measurement for DGPS. Thus, a Base Station was established by keeping the GNSS receiver over the survey pillar for a continuous period of 72 h (31 January 2020 to 2 February 2020) in confirmity with SOI guidelines. However, the base receives signals from all the satellites at least once with 12 h continuous observation. Elevation of the surface ground was measured with reference to the WGS-84 datum level. The base station data were determined in UTM coordinates, which is a mathematical conversion from latitude and longitude to a Cartesian northing and easting (y and x) coordinate system.

The base station was located in the vicinity of weighbridge no. 1. The location of the base station was close to the mining lease boundary and outside the periphery of the ultimate pit plan (located by the mine management) so that it is maintained intact throughout the life of the mine for future reference. The survey of the mining area, comprising three mountains named as blocks A, B and C, was conducted with reference to the established base station coordinates.

Establishment of baselines: In general, survey of a mine is carried out from a single baseline. Reconnaissance survey revealed that a closed traverse from a single baseline would require a large number of settings of short drafts to cover the entire area because of rugged terrain and haphazard old opencast mine workings within the mining lease area. This approach may affect the closing error. Thus, with a

Table 1. Coordinates of primary control points

Base line	Location	Northing (m)	Easting (m)	Elevation (m)	Positional dilution of precision	No. of satellites	Remarks
1	T1	3,197,359.128	583,428.596	390.940	2.51	13	Hilltop temple
	T2	3,197,403.597	583,413.458	361.957	2.15	14	
2	B1	3,197,370.784	585,011.245	211.983	1.57	16	Near base station
	B2	3,197,429.184	584,860.714	212.525	2.14	15	
3	B3	3,196,693.663	585,636.753	216.580	2.79	13	Weigh bridge 3
	B4	3,196,680.126	585,528.738	219.120	2.39	13	
4	B7	3,196,658.545	584,911.654	222.788	1.53	14	Mid of haul road
	B8	3,196,824.254	584,323.436	239.324	1.53	15	
5	F1	3,197,544.101	585,044.526	219.835	1.52	15	Building top
	F1a	3,197,547.464	585,048.876	219.875	1.25	15	
6	7	3,196,807.452	584,327.934	236.899	2.15	15	Weigh bridge 5
	10	3,196,758.798	584,244.954	225.403	2.15	14	

perspective to alleviate the large closing error, baselines were established at suitable locations using GNSS with reference to the same base station. The DGPS observations on primary control points (PCPs) should be made continuously for 2 h if the distance of reference points is within 10 km, according to the guidelines framed by the Chhattisgarh Council of Science and Technology, Raipur, mining lease area[22]. Twelve PCPs were determined at various parts of the mining block through static mode by keeping the rovers over each station for a period of 2 h for the establishment of baselines. Table 1 gives the coordinates of PCPs.

Measurements were conducted with respect to the base station, and the final PCPs were determined after the base and rover data were processed using Trimble Business software. The PCPs were fixed in pairs to establish the baselines. A total of six baselines were established to cover the entire area. Positional dilution of precision (PDOP) ranged between 1.52 and 2.79, indicating good satellite geometry. A PDOP value less than 4 is considered excellent[23]. The number of satellites varied between 13 and 16 during the determination of PCPs.

Establishment of geo-reference stations: The global coordinates of the geo-reference stations were determined from the respective baselines using a total station. The haphazard, old opencast mining all around the foot and at the top of the mountain led to the establishment of a good number of geo-reference stations at short distances to cover the entire surface area to be surveyed. A total of 126 geo-reference stations were fixed to cover all three blocks.

Survey by laser scanner: Point cloud data were generated by setting the TLS over the established geo-reference stations, following the backsight method. Figure 1 provides a few pictorial views of the survey conducted using TLS. After eliminating noise precisely, a topographical mesh was generated by merging all the point cloud data files with the aid of ATLAScan software. Figure 2 is a 3D view of the mine covering the three blocks A–C.

Preparation of contour plan: A surface contour plan was prepared at 10 m intervals based on point cloud data generated by TLS (Figure 3). Measurement by the laser scanner helped generate a precise DEM model of the surface ground profile prior to the commencement of mining. Measurement after periodical excavation using laser technology would help compute the actual volume of the rocks excavated.

Density determination

Both *in situ* density and bulk density of the rocks were determined from the core samples to compute the tonnage of rocks excavated and the amount of broken material left in the mine.

In situ density

In situ density was measured using the standard method given in IS 13030 (ref. 24). Dry density test of the rock samples was conducted in the form of lumps or aggregates of irregular geometry. The method is only used for rocks that do not appreciably swell or disintegrate when oven-dried and immersed in water. Density was calculated using the following relation

$$\rho = \frac{M}{V}, \tag{1}$$

where ρ is the density (kg/m^3), M the mass (kg) and V is the volume of the sample (m^3).

The average density of *in situ* rocks was 2.63 t/m^3. The tonnage computation of *in situ* rocks excavated was done with the average density of the rocks determined.

Bulk density

The bulk density is defined as the mass or weight of a material divided by volume of the material, including voids

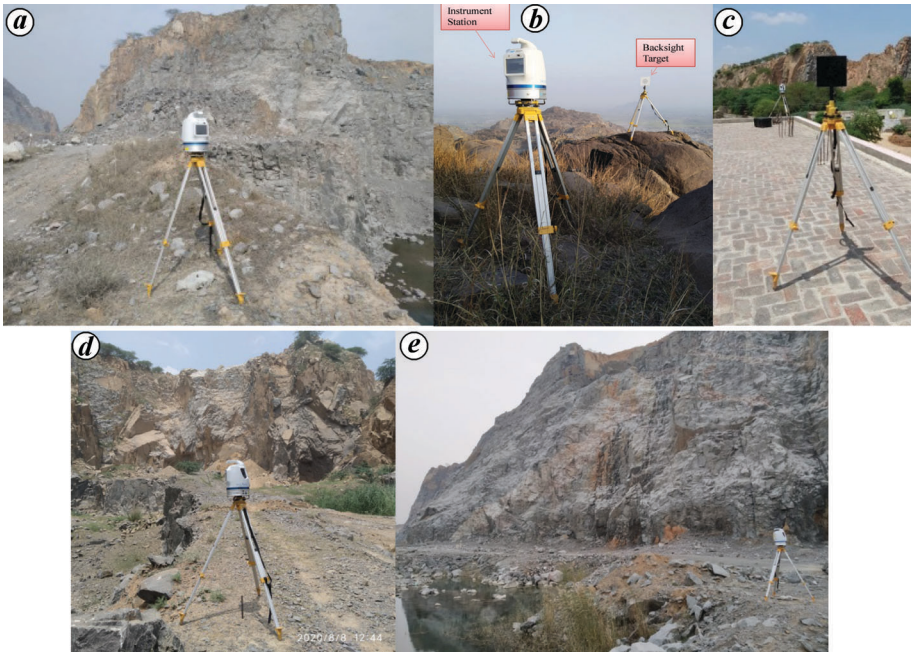

Figure 1. Survey carried out by terrestrial laser scanner.

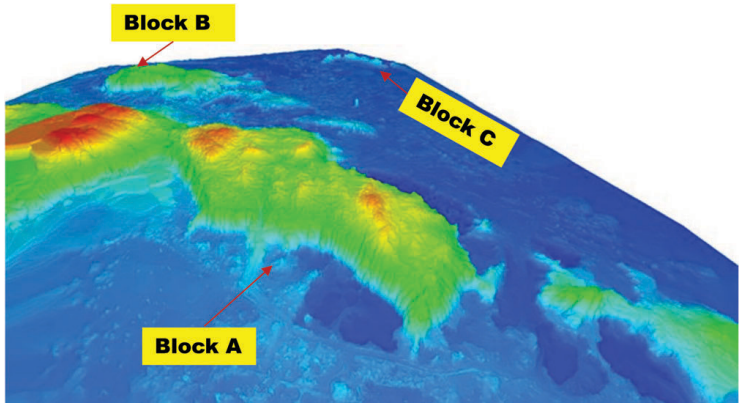

Figure 2. Three-dimensional view of mine showing the location of three blocks.

contained within the volume of a rock, and can be expressed as

$$\rho_B = W_G/V_B, \tag{2}$$

where W_G is the weight/mass of the fragmented material, including crushed fragments, if any, and V_B is the volume of the dumped fragments, including internal voids between fragments/crushed material.

The blasted muck is transported by dumpers/trucks to the required stockyards. Since bulk density and *in situ* density are not similar, the former was necessary to evaluate the actual quantity of material transported by dumpers/trucks. Core samples were used to determine bulk density in the laboratory. No ASTM standard is available to determine the bulk density of a rock core sample. A methodology has been preluded with a rational approach through laboratory examination to determine the bulk density of rocks excavated in the Khanak Stone Mine.

Methodology

Large-sized rock samples collected from the mine were cored to various lengths. The volume (V_1) of each core sample was determined by taking the average diameter and average length measured, and density was determined by dividing dry mass (M) by volume following the ISRM standard.

Each core sample was thereafter broken into pieces in four steps, each with a different fragment size. The broken samples were kept together for each step, and photographs were taken at each stage. Photographs were taken along

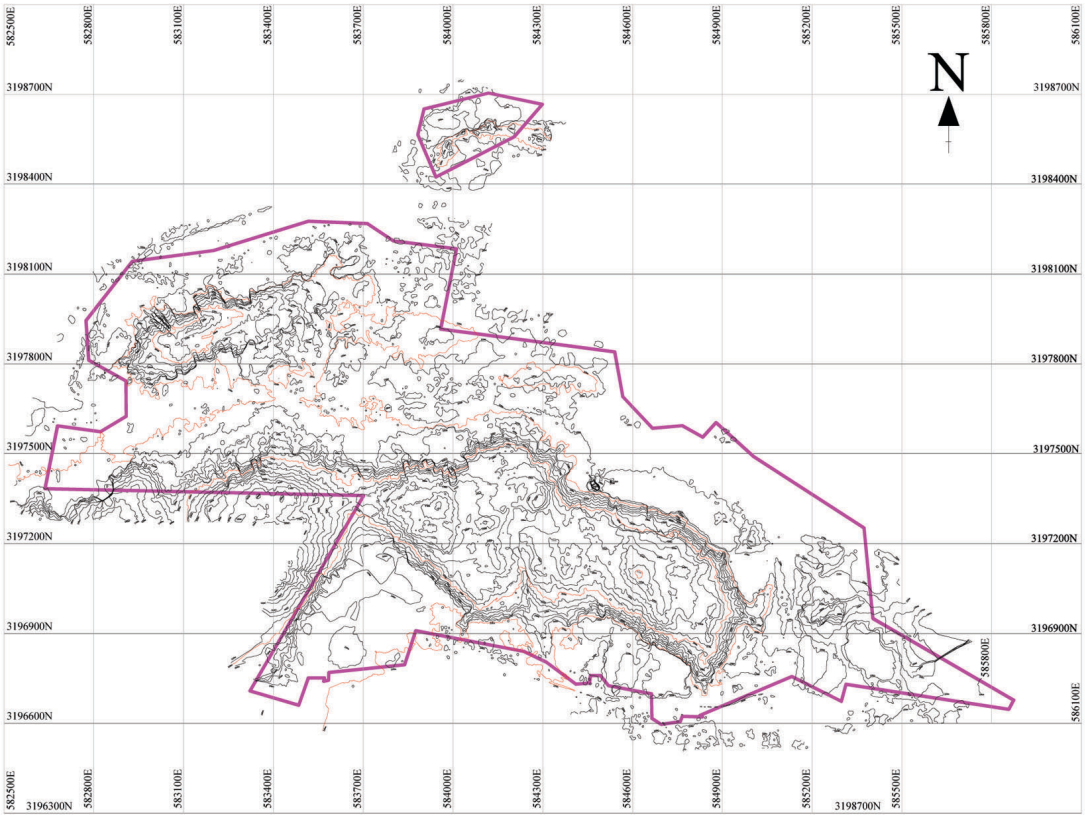

Figure 3. Surface contour of the mine at 10 m interval.

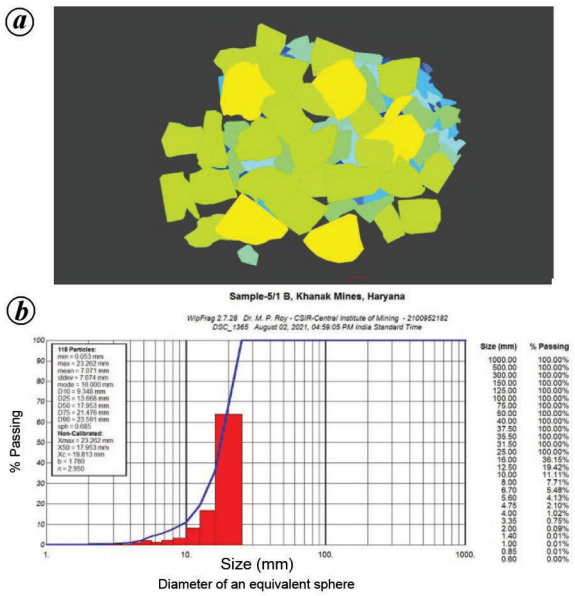

Figure 4. Determination of fragment size of rocks. (***a***) Image analysis. (***b***) Particle size distribution.

with the measuring scale to determine the actual fragment size through WipFrag software as shown in Figure 4.

WipFrag (M/s Wipware Inc, Canada) is an image analysis software that examines digital images of broken rocks with a granulometry system to predict grain size distribution in the muck pile. Photographs of the broken rock images are transformed into a particle map or network. WipFrag allows comparing the automatically generated net against the rock image. The fragment boundaries are analysed efficiently using edge detection variables (EDVs). Any inaccuracies can be corrected by manual editing with a mouse to improve edge detection.

The output of the analyses is in the form of a number of exposed fragmented blocks expressed in different percentile sizes, viz. D_{10}, D_{25}, D_{50}, D_{75} and D_{90}. For achieving the mean size of the fragments, D_{50} is chosen, which indicates the size of the sieve opening through which 50% by size of the sample would pass.

In any muck pile of the fragmented rock mass, two types of voids exist in the broken samples, namely surface pore void (SPV) and inter-particle/fragment void (IPV). According to Crawford[25], internal pores should only be considered to determine bulk density. Hence, SPV should be removed while determining bulk density in the laboratory. The steps followed to remove the SPV are detailed below.

The volume (V_2) of the broken samples, including inter-particle voids and SPV, is measured at each stage with the help of a measuring cylinder (Figure 5). Volume of the surface pore is determined by the measuring cylinder (Figure 6). Assuming a constant SPV size throughout the inner surface of a cylinder, radius (r_1) and height (h_1) are

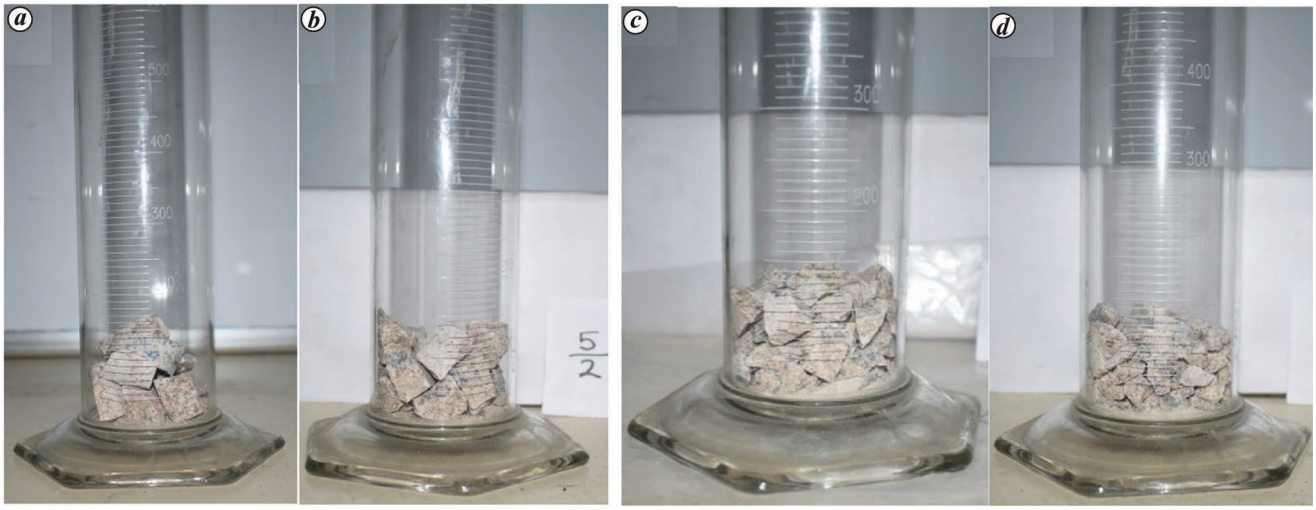

Figure 5. Measurement of volume for different chip sizes. (***a***) Stage 1, (***b***) stage 2, (***c***) stage 3 and (***d***) stage 4.

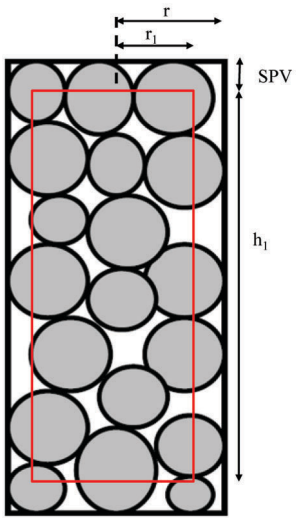

Figure 6. Dimensions for the determination of inter-particle/fragment void.

calculated to determine the volume (V_3) containing only the inter-particle void, expressed as

$$V_3 = \pi r_1^2 h_1, \tag{3}$$

$$\text{Total void} = V_2 - V_1 = V_{ot}. \tag{4}$$

Inter-particle void is computed as

$$V_{oip} = (V_{ot} \times V_3)/V_1. \tag{5}$$

$$\text{Bulk density} = V_1 + V_{oip}, \tag{6}$$

where r is inner radius of the cylinder, r_1 the radius of the inter-particle void and h_1 is the height of the inter-particle void.

Bulk density is determined for different chip sizes, and the relation between bulk density and chip size is established.

The average size of the actual boulder, after blasting, is also determined in the same process using WipFrag (Figure 7).

The best-fit curve is plotted between bulk density and chip size of the rocks determined in the laboratory. Actual bulk density of the rocks is determined based on the boulder size obtained after blasting, using the established relation.

Results

A number of cores were prepared from the rock samples collected from different parts of the mine. The best-fit relation was developed between chip size and bulk density, expressed as (Figure 8).

$$BD = 2.4873 \times CS^{(-0.0035)}, \tag{7}$$

where BD is the bulk density (t/m^3) and CS is the chip size (cm).

The shape and size of the rocks affect the empty space between them and consequently influence bulk density. Thus, relation between bulk density and chip size was developed because of the influence of irregular geometry of the broken chips. However, a few incongruous data were eliminated to arrive at the trend, and the best-fit relationship was established. The average size of the boulders was around 20–30 cm. Thus, using eq. (7), the bulk density was found to be 2.46 t/m^3, which is also in close agreement with that mentioned in the mining plan (2.45 t/m^3).

Volume computation

The initial survey was carried out prior to the commencement of mining, and the last measurement was conducted

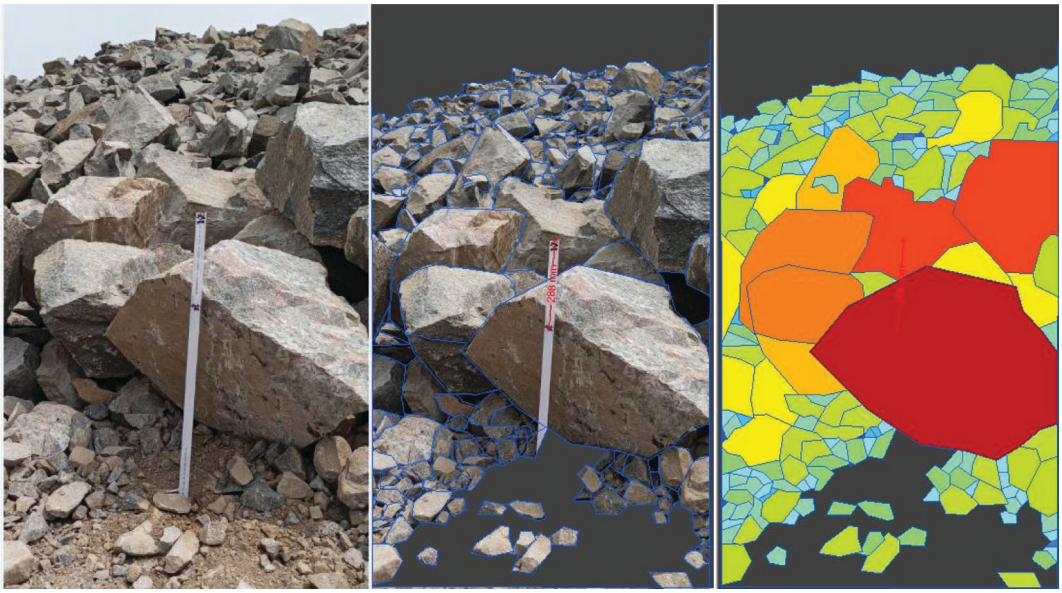

Figure 7. Determination of boulder size after blasting using WipFrag software.

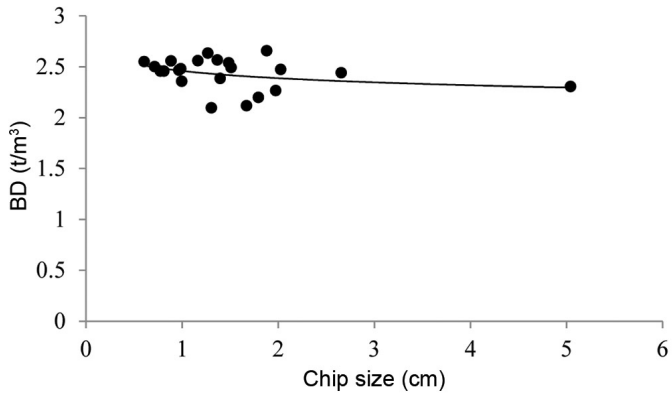

Figure 8. Relation between bulk density (BD) and chip size of rocks.

at the end of March 2021 and continued till the first week of April, i.e. up to 6 April 2021, to compute the volume of rocks excavated till the financial year 2021. Rock excavation was done from blocks A and B. Excavations were done in both blocks for the development of the mine, i.e. haul road development up to the top of the hills, etc.

Raw data obtained from the laser scanner contain noisy point clouds. Noisy data are generated due to sun rays, trees, vehicles, etc. Noise leads to a negative influence on the application of laser scanning data, and hence, it should be eliminated before processing the data to achieve the precise surface profile. Hence, volume computation was done after removing noise using ATLAScan software.

Methodology

To compute the volume of any irregular mass of earthwork, it is necessary to obtain the sectional area of each cross-section. Hence, cross-sections are prepared at every 10 m interval. Reduced level (RL) data are generated at every 1 m interval along each section from the interpolated digital terrain model. RL profiles of all the measurements are plotted. Area of actual excavation along each section is computed using AutoCAD. The volume of rocks excavated between two sets of measurements is calculated by the widely accepted trapezoidal rule, expressed as

$$V = \frac{D}{2}\{A_1 + A_n + 2(A_2 + A_3 \ldots\ldots + A_{n-1})\}, \tag{8}$$

where V is the volume (m^3), D the common distance between two sections (m), A_1 the area of the first section (m^2), A_n the area of the last section (m^2) and A_2 to A_{n-1} is the area of the intermediate sections (m^2).

No limitation of this rule and its applications for any number of sections are the advantages of this method.

Table 2. Computation of tonnage excavated

Sl. no.	Parameters	Block-A	Block-B	Remarks
A	Total cut (m^3)	1,644,029.6	271,613.92	
B	Density of rocks (t/m^3)	2.63	2.63	*In situ* density
C	Tonnage cut (t)	4,323,797.8	714,344.6	A × B
D	Total fill (m^3)	683,838.2	34,595.71	
E	Bulk density of rocks (t/m^3)	2.46	2.46	Bulk density
F	Tonnage fill (t)	1,682,242	85,105.455	D × E
G	Tonnage produced (t)	2,641,555.9	629,239.15	C – F
H	Total tonnage produced (t)	3,270,795.024		Sum of G of blocks A and B
I	Tonnage dispatched till 6 April 2021	3,237,412.175		
J	Percentage deviation	1.02		

Volume calculation

Cross-sections were prepared in the north–south direction at an interval of 10 m for both blocks A and B. Broken rocks were filled at different locations in both blocks for the development of haul roads from the foot of the hill to the top and for levelling the ground. Weathered and poor-quality rocks with soil materials were also dumped at the side of the hill. Excavations were observed in 176 sections (125 in block A and 51 in block B). A few intermediate sections showed no excavation as mining was done at different locations. Area of excavation along each section was computed using AutoCAD. The hatch portion in red indicates the area of excavation along that section, whereas the blue shade indicates the fill. Volume of excavation was computed using eq. (8). Table 2 gives the volume excavated from the commencement of mining till April 2021. Some variation in tonnage is anticipated due to the cumulative effect of the following: (a) Heterogeneity of the rocks leading to density variation. In places, rocks were weathered (poor-quality rocks), containing soil whose overall density is likely to be less. However, an average *in situ* density of 2.63 t/m^3 was considered for volume computation in tonnage. (b) Prior to the commencement of mining, loose/broken rocks were also dumped at random places, whose accountability in isolation cannot be done by laser measurements. This also affects the average density of the rocks. (c) Limitation in determining the bulk density of rocks using standard methods.

Conclusion

GNSS proved pivotal for precisely surveyingintricate topography in the mining arena. The establishment of the base station and PCPs at different locations using GNSS enabled the precise survey of the entire mine. Integration of GNSS and TLS played an invaluable role in preparing a precise surface contour plan. *In situ* density and bulk density of rocks of Khanak Stone Mine determined in the laboratory were 2.63 and 2.46 t/m^3 respectively. The total volume of rocks excavated from the inception of mining was computed using a trapezoidal rule amounting to 3,270,795.024 t. The amount of rocks dispatched was 3,237,412.175 t according to the record provided by the mine management. The percentage variation from the actual tonnage dispatched was 1.02, within the acceptable range.

Thus, the challenges of surveying difficult topography can be overcome by applying modern technology. The hybrid of GNSS and TLS has immense potential for survey of any profile of topography except forest land covered by large trees.

1. Heinrichs, G. *et al.*, A hybrid Galileo/UMTS receiver architecture for mass-market applications, GNSS. 2005; http://www.gawain-receivers.com/publications/IfEN_Paper_GAWAIN_GNSS2005.pdf.
2. Leick, A., Rapoport, L. and Tatarnikov, D., *GPS Satellite Surveying, 4th edn*, John Wiley, NJ, USA, 2015, pp. 1–840.
3. Pini, M., Falco, G. and Presti, L. L., Estimation of satellite-user ranges through GNSS code phase measurements. In *Global Navigation Satellite Systems Signal – Theory and Applications* (ed. Jin, S.), InTech, Rijeka, Croatia, 2012.
4. Yuwono, H. E. Y., Cahyadi, M. N., Rahmadiansah, A., Yudha, I. S. and Sari, A., Assessment of the single frequency low cost GPS RTK positioning. In *Proceedings of the IOP Conference Series: Earth and Environmental Science, Volume 280*, IOP Publishing, Bristol, UK, 2018.
5. Liu, G. and Lachapelle, G., Ionosphere weighted GPS cycle ambiguity resolution. In *Proceedings of the U.S. Institute of Navigation National Technical Meeting*, San Diego, CA, USA, January 2002, pp. 889–899.
6. Sieradzki, R. and Paziewski, J., On the feasibility of interhemispheric patch detection using ground-based GNSS measurements. *Remote Sensing*, 2018, **10**(12), 2044; doi:10.3390/rs10122044.
7. Wielgosz, P., Hada, T., Kłos, A. and Paziewski, J., Research on GNSS positioning and applications in Poland in 2015–2018. *Geod. Cartogr*., 2019, **68**(1), 87–119.
8. Hegarty, C. J. and Chatre, E., Evolution of the global navigation satellite system (GNSS). *Proc. IEEE*, 2008, **96**(12), 1902–1917.
9. Catania, P., Comparetti, A., Febo, P., Morello, G., Orlando, S., Roma, E. and Vallone, M., Positioning accuracy comparison of GNSS receivers used for mapping and guidance of agricultural machines. *J. Agron*., 2020, **10**, 924; doi:10.3390/agronomy10070924.
10. Gokhan, G. and Jin, S., Evaluation of ocean tide loading effects on GPS-estimated precipitable water vapour in Turkey. *Geod. Geodyn*., 2016, **7**(1), 32–38.
11. Casula, G., Geodynamics of the Calabrian Arc area (Italy) inferred from a dense GNSS network observations. *Geod. Geodyn*., 2016, **7**(1), 76–86.
12. Kostyanev, S. *et al.*, The use of GNSS technologies for application in mining, geology and geodesy in Bulgaria. In XIX Congress of the Carpathian–Balkan Geological Association Thessaloniki, Greece, 23–26 September 2010, p. 206.

13. Vrublová, D., Kapica, R., Gibesová, B., Mudruňka, J. and Struś, A., Application of GNSS technology in surface mining. *Geod. Cartogr*., 2016, **42**(4), 122–128; doi.org/10.3846/20296991.2016.1268433.
14. Kumar, P., Chaudhary, S. K., Shukla, G. and Kumar, S., Assessment of positional accuracy of DGPS: a case study of Indian School of Mines Dhanbad, Jharkhand, India. *Int. J. Adv. Earth Sci*., 2013, **2**(1), 1–7.
15. Nehra, T., Carrying DGPS survey and preparation of digital elevation model. *Int. J. Curr. Eng. Sci. Res.*, 2017, **4**(10), 144–148.
16. El-Rabbany, A., *Introduction to GPS: The Global Positioning System*, Artech House Publishers, Norwood, MA, 2002, p. 176.
17. Ahamad, N. and Ojha, S. K., The practical application of laser scanning in a mining environment. In Second National Conference on Mining Equipment: New Technologies, Challenges and Applications, Indian School of Mines, Dhanbad, 2015.
18. Van der Merwe, J. W. and Andersen, D. C., Applications and benefits of 3D laser scanning for the mining industry. *J. S. Afr. Inst. Min. Metall*., 2013, **113**(3), 213–219.
19. Smith, M. W., Direct acquisition of elevation data: Terrestrial Laser Scanner. In *Geomorphological Techniques*, British Society for Geomorphology, London, UK, 2015, p. 14.
20. Buckley, S. J., Howell, J. A., Enge, H. D. and Kurz, T. H., Terrestrial laser scanning in geology: data acquisition, processing and accuracy considerations. *J. Geol. Soc.*, 2008, **165**(3), 625–638.
21. Bazarnik, M., Slope stability monitoring in open pit mines using 3D terrestrial laser scanning. In Fourth International Conference on Applied Geophysics, E3S Web of Conferences 66, 2018, 01020; https://doi.org/10.1051/e3sconf/20186601020.
22. Anon., Guidelines for DGPS survey for mining lease/forest diversion and compensatory afforestation for verification and authentication at CGSAC. Chhattisgarh Council of Science and Technology, 2020, p. 9.
23. Anon, *Handbook of Topography*, Survey of India, 2009, p. 137; http://www.iism.nic.in/Documents/soichapter-xi.pdf.
24. BIS, Method of test for laboratory determination of water content, porosity, density, and related properties of rock material – IS 13030:1991. Bureau of Indian Standards, New Delhi, 1991.
25. Crawford, K. M., Determination of bulk density of rock core using standard industry methods. Master's report, Michigan Technological University, USA, 2013; https://doi.org/10.37099/mtu.dc.etds/661.

ACKNOWLEDGEMENTS. We acknowledge the support received from the mining industry for facilitating field investigation and data collection. We thank the Director, CSIR-Central Institute of Mining and Fuel Research, Dhanbad, for permission to publish this paper. The views expressed here are those of the authors and not necessarily of the organization they represent.

Received 7 March 2023; revised accepted 30 October 2023

doi: 10.18520/cs/v126/i3/336-344